


## Hyperbolic blockade: Photonic density of states and spontaneous emission rate at the interface with a conducting medium

Evgenii E. Narimanov

*School of Electrical and Computer Engineering and Birck Nanotechnology Center, Purdue University, West Lafayette, Indiana 47907, USA*

 (Received 25 March 2018; revised manuscript received 18 June 2018; published 5 July 2018)

The surface scattering of free electrons strongly modifies the electromagnetic response near the interface. Due to the inherent anisotropy of the surface scattering that necessarily reverses the normal to the interface component of the electron velocity while its tangential component may remain the same, a thin layer near a high-quality interface shows strong dielectric anisotropy. The formation of the resulting hyperbolic dispersion layers near the metal-dielectric interface strongly modifies the local density of states, and leads to orders of magnitude changes in all associated phenomena.

DOI: [10.1103/PhysRevB.98.041401](https://doi.org/10.1103/PhysRevB.98.041401)

Light incident on a conducting material changes the dynamics of the free charge carriers near the interface. The resulting surface plasmon-polariton excitations [1] increase the local photonic density of states, leading to a dramatic change in a broad range of related phenomena—from the enhancement of the spontaneous emission rates near the interface [2], to surface-enhanced Raman scattering [3], to subwavelength light localization and confinement [1]. While most of these phenomena can be understood, at least at the qualitative level, within the framework of the effective local dielectric permittivity of the metal, this approach becomes progressively more problematic when the plasmon fields change on a scale that is compatible to the electron mean free path. The importance of an accurate account of the inherent mobility of free charge carriers is now well understood [4–7], and the corresponding “spatial dispersion” formalism was successfully used for a quantitative description of surface plasmon polaritons in metallic nanostructures [4–7].

However, the inherent mobility of the free charge carriers not only leads to an essentially nonlocal theoretical description (the fundamental property which is equally important both at the bulk and near the surface of the conducting medium), but also qualitatively changes the nature of the electromagnetic response near the metal-dielectric interface. For a high-quality surface, the electron reflection will reverse normal to the surface component of the momentum, while leaving its tangential projection intact. As a result, while the specular reflection at the interface will not strongly affect the electromagnetic response in the tangential direction, its component that is normal to the metal surface will be substantially altered. Even in the presence of substantial surface roughness [8], the effect of the surface scattering on the momentum transfer from the free carriers to the interface (and thus the entire sample as a whole) is still very different in the normal and tangential directions. As a result, the free carrier electromagnetic response near the conductor-dielectric interface will show strong anisotropy.

In this thin interfacial layer, while a diffuse component of the surface scattering leads to an increased loss, the tangential dielectric permittivity retains its negative sign. However, the electronic contribution to the normal to the interface

permittivity is strongly suppressed (as the free carrier current density at the interface in this direction is exactly zero, regardless of the magnitude of the electric field). As a result, the interface layer has an essentially hyperbolic electromagnetic response.

The formation of the hyperbolic layer near the metal-dielectric interface will no longer support direct resonant coupling from the incident field to the free electrons in the “bulk” metal, leading to a suppression of the conventional plasmon resonance via the *hyperbolic blockade*. While the conventional surface plasmon-polariton mode is still present in the system, it can no longer reach the extreme values of the wave numbers predicted for a “direct” (lossy) metal-dielectric interface. At the same time, the hyperbolic layer leads to an additional surface wave, the so-called “hyperplasmon,” that can now coexist with the standard plasmon polariton [9].

As a result, the local photonic density of states (PDOS) at the metal-dielectric interface is strongly modified. First, the peak near the surface plasmon resonance frequency is strongly suppressed, and the corresponding density of states is substantially reduced, while at other frequencies when the hyperplasmon waves are present, it can be substantially enhanced. Second, the photonic density of states now shows a very different behavior as a function of the distance to the metal-dielectric interface  $d$ . When it is much larger than the thickness of the hyperbolic layer  $d_*$ , the latter is not “resolved”—and the density of states is close to the value calculated from the “bulk” properties of the metal (albeit with the nonlocal corrections [4]). However, for  $d \leq d_*$ , it is now the hyperbolic layer that determines the density of states, leading to a crossover to a different behavior.

In the quantitative theory of this Rapid Communication, we focus on the calculation of the spontaneous emission rate for a small emitter (such as a dye molecule or a quantum dot) in proximity to the metal-dielectric interface. While directly connected to the local density of states via the Fermi golden rule, and thus offering a probe into the local PDOS, the spontaneous emission rate is also an important quantity for both the interpretation of experimental data [10–12] and for technological applications [13].

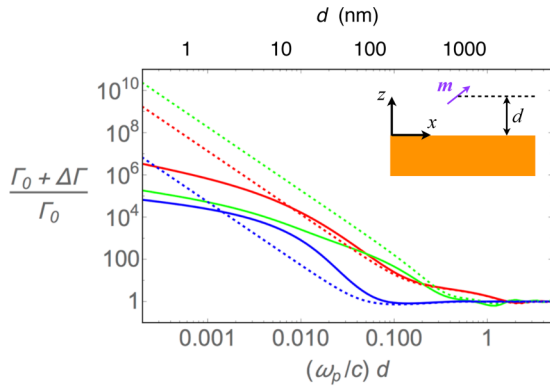


FIG. 1. The spontaneous emission rate near the dielectric-conductor interface, as a function of the distance  $d$  from the emitter to the surface (see the inset). The emission rate is normalized to its value in infinite dielectric  $\Gamma_0$ . Solid lines show the exact solution obtained in the present work, while the corresponding dotted lines represent the results of the calculation based on the local theory. Different colors correspond to different frequencies and emission polarizations: The dipole moment  $\mathbf{m} \parallel \hat{\mathbf{n}}$  at  $\omega = 0.5\omega_{\text{sp}}$  (red),  $\mathbf{m} \perp \hat{\mathbf{n}}$  at  $\omega = \omega_{\text{sp}}$  (green),  $\mathbf{m} \parallel \hat{\mathbf{n}}$  at  $\omega = 2\omega_{\text{sp}}$  (blue), where  $\omega_{\text{sp}}$  is the surface plasmon resonance frequency and  $\hat{\mathbf{n}}$  is a unit vector along the normal to the interface. In this calculation, the electron scattering time  $\tau = 18.84/\omega_p$ , the crystal lattice permittivity of the conductor  $\epsilon_\infty = 12.15$ , the permittivity of the dielectric  $\epsilon_d = 10.23$ , and the Fermi velocity  $v_F = 0.00935c \simeq 2.8 \times 10^6$  m/s; for the plasma wavelength  $\lambda_p \equiv 2\pi c/\omega_p = 10 \mu\text{m}$ , these parameters correspond to the AlInAs/InGaAs material system of Ref. [29].

In the weak-coupling limit [2,14], for an emitter located at the distance  $d$  from a planar interface (see Fig. 1), we obtain

$$\Gamma = \Gamma_0 + \eta \Delta\Gamma, \quad (1)$$

with

$$\Delta\Gamma = \frac{3c^3}{4|\mathbf{m}|^2\omega^3\epsilon_d^{3/2}} \text{Re} \int_0^\infty \frac{dk k}{k_z} \exp(2ik_z d) \times [r_s m_\tau^2 (k^2 + k_z^2) - r_p (m_\tau^2 k_z^2 - 2m_n^2 k^2)], \quad (2)$$

where  $\eta < 1$  is the quantum efficiency [14] that accounts for other (nonradiative) decay channels of the excited state in the emitter,  $k_z \equiv \sqrt{\epsilon_d(\omega/c)^2 - k^2}$ ,  $\omega$  is the emitted light frequency, and  $\epsilon_d$  is the permittivity of the dielectric medium at  $z > 0$ , while  $m_\tau$  and  $m_n$  are the tangential and normal to the metal-dielectric interface projections of the unit vector  $\mathbf{m}$  that indicates the direction of the dipole moment of the emitter (see the inset to Fig. 1). Note that Eqs. (1) and (2) define the total radiative linewidth that includes both the far-field emission and the radiation into the lossy modes of the metal-dielectric interface. Unless special measures are taken to outcouple the latter back into the free space, the emission into lossy modes leads to the Joule heating of the sample, while the detected far-field intensity corresponds to only a fraction of the total radiative linewidth (1) and (2).

We emphasize that (1) and (2) imply no assumption on the nature of the material on the other side of the interface: The medium can be metallic, hyperbolic, or dielectric, with either a local or nonlocal electromagnetic response, as long as it has translational symmetry parallel to the interface, and at least a

uniaxial symmetry along the normal to the surface. Under these conditions, the incident  $s$  and  $p$  polarizations are not mixed up upon reflection, and can be described by the corresponding reflection amplitudes  $r_s$  and  $r_p$ .

The original mathematical formalism for the description of the electromagnetic field reflection from free charge carriers [8,15,16] was developed in the context of the anomalous skin effect [17,18], when the electron mean free path is longer than the effective “skin depth” [8]. However, in optical experiments with plasmonic media at room temperatures, the field penetration depth generally exceeds the electronic mean free path [19], which does not allow a direct application of these results to plasmonic systems.

When the distance to the interface  $d$  is much larger than de Broglie wavelength of the free charge carriers,

$$d \gg \lambda, \quad (3)$$

the integral in (2) is dominated by the waves with in-plane wave numbers  $k \leq 1/d \ll 1/\lambda$ . The free charge carrier response at such wave numbers can be treated within the semiclassical framework, via the Boltzmann kinetic equation [8]

$$\frac{\partial f_{\mathbf{p}}}{\partial t} + \mathbf{v}_{\mathbf{p}} \cdot \nabla f_{\mathbf{p}} + e\mathbf{E} \cdot \mathbf{v}_{\mathbf{p}} \frac{\partial f_0}{\partial \epsilon_{\mathbf{p}}} = -\frac{f_{\mathbf{p}} - f_0}{\tau}, \quad (4)$$

where  $f_{\mathbf{p}}(\mathbf{r}, t)$  is the charge carrier’s distribution function with its equilibrium (Fermi-Dirac) limit  $f_0$ ,  $\epsilon_{\mathbf{p}}$  is the electron energy for the (Bloch) momentum  $\mathbf{p}$ ,  $\mathbf{v}_{\mathbf{p}} \equiv \partial \epsilon_{\mathbf{p}} / \partial \mathbf{p}$  is the corresponding electron group velocity, and  $\tau$  is the effective relaxation time defined by the bulk scattering (due to, e.g., phonons, impurities, etc.). The local equilibrium distribution function  $f_0$  is defined by the actual time-dependent local density rather than its time-averaged value [20], if the scattering process does not locally create or annihilate charge carriers. However, when the electromagnetic field frequency  $\omega \gg 1/\tau$ , the local correction to the equilibrium distribution function can be neglected [21,22].

For a high-quality interface along one of the symmetry planes of the crystal, the surface leads to specular reflection of the charge carriers [8], which can be accounted for by the boundary condition on the distribution function [8,15,16,23,24],

$$f_{\mathbf{p}^-}(\mathbf{r}_s) = f_{\mathbf{p}^+}(\mathbf{r}_s), \quad (5)$$

where  $\mathbf{r}_s$  corresponds to any point at the interface, and  $\mathbf{p}^+$  and  $\mathbf{p}^-$  are connected by the specular reflection condition.

The electromagnetic field in the system is defined by the self-consistent solution of the kinetic equation and the surface scattering boundary condition together with the Maxwell equations. The corresponding electron charge and current densities are then given by

$$\rho(\mathbf{r}) = 2 \int \frac{d\mathbf{p}}{(2\pi\hbar)^3} \cdot [f_{\mathbf{p}}(\mathbf{r}) - f_0(\epsilon_{\mathbf{p}})], \quad (6)$$

$$\mathbf{j}(\mathbf{r}) = 2 \int \frac{d\mathbf{p}}{(2\pi\hbar)^3} \cdot e \mathbf{v}_{\mathbf{p}} f_{\mathbf{p}}(\mathbf{r}). \quad (7)$$

Following the mathematical approach described in Ref. [9], this problem can be solved exactly, and for the reflection

coefficient in the  $s$  polarization we obtain

$$r_s = -1 + 2k_z(k_z + \sqrt{\epsilon_\tau(k) \cdot (\omega/c)^2 - k^2})^{-1}, \quad (8)$$

where

$$\epsilon_\tau(k) = \epsilon_\infty + \frac{2e^2}{\pi^2 \hbar^3 \omega} \int \frac{d\mathbf{p} v_y^2}{\omega + kv_y + i/\tau} \cdot \frac{\partial f_0}{\partial \epsilon_{\mathbf{p}}}. \quad (9)$$

For a degenerate electron gas the integration in (9) yields

$$\epsilon_\tau(k) = \epsilon_\infty - \frac{\epsilon_\infty \omega_p^2}{\omega(\omega + i/\tau)} \mathcal{F}_\tau \left( \frac{v_F k}{\omega + i/\tau} \right), \quad (10)$$

with

$$\mathcal{F}_\tau(x) = \frac{3}{x^2} [\mathcal{F}_0(x) - 1], \quad \mathcal{F}_0(x) = \frac{1}{2x} \log \frac{1+x}{1-x}, \quad (11)$$

where  $v_F$  is the electron Fermi velocity,  $\epsilon_\infty$  is the “background” permittivity of the crystal lattice in the conductor, and  $\omega_p$  is the standard plasma frequency [1]. Note that the expression  $\epsilon_\tau(k)$  in Eq. (10) is consistent with the other models of nonlocal free carrier responses used in the recent literature [4,25].

For the  $p$  polarization, we find

$$r_p = -1 + 2k_z \left( k_z + \frac{2i\epsilon_d \omega^2}{\pi c^2} \int_0^\infty \frac{dq}{D(k,q)} \right)^{-1}, \quad (12)$$

where

$$D(k,q) = \epsilon_x(k,q) \frac{\omega^2}{c^2} - q^2 - \frac{v_{xz}^2(k,q)}{\epsilon_z(k,q) \frac{\omega^2}{c^2} - k^2}, \quad (13)$$

and

$$\begin{aligned} \epsilon_{x,z}(k,q) &= \epsilon_\infty - \frac{16\pi i e^2 \tau}{\omega} \int_{v_z > 0} \frac{d\mathbf{p}}{(2\pi \hbar)^3} \frac{\partial f_0}{\partial \epsilon_{\mathbf{p}}} \\ &\quad \times v_{x,z}^2 \frac{1 - i\omega\tau + ikv_x\tau}{(1 - i\omega\tau + ikv_x)^2 + q^2 v_z^2 \tau^2}, \quad (14) \\ v_{xz}(k,q) &= kq - \frac{16\pi e^2 \tau^2 \omega q}{c^2} \int_{v_z > 0} \frac{d\mathbf{p}}{(2\pi \hbar)^3} \frac{\partial f_0}{\partial \epsilon_{\mathbf{p}}} \\ &\quad \times v_x v_z^2 \frac{1}{(1 - i\omega\tau + ikv_x\tau)^2 + q^2 v_z^2 \tau^2}. \quad (15) \end{aligned}$$

For a degenerate electron gas [26], analytical integration over the electron momentum  $\mathbf{p}$  reduces Eqs. (14) and (15) to

$$\begin{aligned} \epsilon_x(k,q) &= \epsilon_\infty - \frac{3\epsilon_\infty \omega_p^2}{2} \frac{1 + i/(\omega\tau)}{v_F^2} \left\{ \frac{q^2 - 2k^2}{k^2 + q^2} \right. \\ &\quad \left. + \left( \frac{v_F^2 q^2}{(\omega + i/\tau)^2} + \frac{2k^2 - q^2}{k^2 + q^2} \right) \mathcal{F}_0 \left( \frac{v_F \sqrt{k^2 + q^2}}{\omega + i/\tau} \right) \right\}, \quad (16) \end{aligned}$$

$$\epsilon_z(k,q) = \epsilon_x(q,k), \quad (17)$$

$$\frac{v_{xz}(k,q)}{kq} = 1 + \frac{9\epsilon_\infty}{2(1 + \frac{i}{\omega\tau})} \frac{\mathcal{F}_v \left( \frac{v_F \sqrt{k^2 + q^2}}{\omega + i/\tau} \right)}{(k^2 + q^2)c^2/\omega_p^2}, \quad (18)$$

where

$$\mathcal{F}_v(x) = \frac{1}{x^2} + \left( \frac{1}{3} - \frac{1}{x^2} \right) \mathcal{F}_0(x). \quad (19)$$

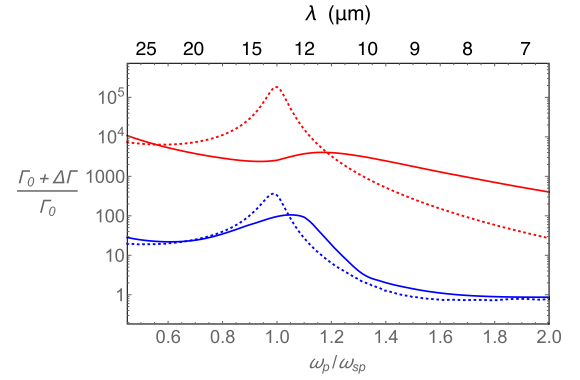


FIG. 2. The frequency dependence of the spontaneous emission rate near the conductor-dielectric interface. As in Fig. 1, solid lines show the exact solution, while the dotted curves correspond to the calculations using the local response model, for  $\mathbf{m} \parallel \hat{\mathbf{n}}$  at  $d = 0.01c/\omega_p$  (red) and  $d = 0.1c/\omega_p$  (blue). The material parameters are the same as in Fig. 1. Note the suppression of the plasmon resonance due to the hyperbolic blockade, together with an order of magnitude enhancement of the spontaneous emission rate above the plasmon resonance frequency, seen for  $d = 0.1c/\omega_p$  (red curve).

Together, Eqs. (12) and (16)–(19) define the reflection coefficient  $r_p$ .

The electromagnetic field near the interface with a conducting medium can also be represented in terms of the surface impedance  $Z$  that defines the ratio of the tangential components of the electric and magnetic fields at the interface [8,15,16,21]. The values of  $Z$  for the  $s$  and  $p$  polarizations calculated from Eqs. (8)–(19) are consistent with the earlier results of Kliewer and Fuchs [21], up to a small correction [22] only relevant at low frequencies ( $\omega \ll 1/\tau$ ) that originates from a difference in the representations of the collision integral in the kinetic equation (4).

The resulting spontaneous emission rate can be calculated by substituting our analytical expressions for the reflection coefficients  $r_s$  and  $r_p$  into the general equation (2). In Fig. 1 we compare the resulting values (solid lines) with the predictions of the standard local theory (dashed lines) that describe the conductor as an effective medium with the (Drude) permittivity  $\epsilon_m(\omega) = \epsilon_\infty(1 - \frac{\omega_p^2}{\omega(\omega + i/\tau)})$ . As the distance to the interface is reduced, the local approximation initially underestimates the density of states, which is consistent with the results of Ref. [4]. However, at a smaller distance  $d < d_*$ , this behavior is reversed: The actual density of states is now smaller than the local estimate. This is the result of the hyperbolic blockade: The hyperbolic layer “blocks” the coupling to conventional surface plasmon polaritons, and the photonic density of states is reduced. Also note the strong frequency dependence of  $d_*$ : The distance corresponding to the crossover between the two different regimes nonmonotonically changes with the electromagnetic wavelength.

The frequency dependence of the spontaneous emission rate for a given distance to the interface, presented in Fig. 2, shows further evidence of the hyperbolic blockade. Note the suppression of the plasmon resonance, especially at the smaller distance to the interface. Furthermore, the coupling to hyperplasmons—the new surface waves that originate from

the hyperbolic layer [9]—manifests itself in the enhancement of the spontaneous emission rate, seen in Fig. 2 at higher frequencies.

This behavior should be contrasted to the prediction of the existing theories of spontaneous emission near an interface of a nonlocal medium [27]. While starting from the surface impedance approach [15,16,21] that also relies on a semiclassical framework, the authors of Ref. [27] then introduced the hydrodynamic approximation that does not accurately account for the hyperplasmon modes [9]. As a result, aside from the quantitative inaccuracy of the spontaneous emission rate at small distances to the interface, the predictions of Ref. [27] were limited to the reduction of the width of the excited state due to spatial dispersion.

When the distance from the emitter to the interface is much smaller than the free-space wavelength,  $d \ll \lambda_0$ , the analytical expression for the spontaneous emission rate can be reduced to

$$\begin{aligned} \Delta\Gamma = & \frac{3}{4}\Gamma_0 \frac{m_\tau^2 + 2m_n^2}{|\mathbf{m}|^2} \frac{\epsilon_\infty}{\sqrt{\epsilon_d(\epsilon_d + \epsilon_\infty)^2}} \left(\frac{c}{v_F}\right)^2 \left(\frac{\omega_p}{\omega}\right)^2 \\ & \times \left\{ \frac{3}{2\omega\tau} \frac{c}{\omega d} + \frac{c}{v_F} \frac{\epsilon_d + \epsilon_\infty}{\epsilon_d + \epsilon_m(\omega)} \operatorname{Im} \left[ \left(1 + \frac{i}{\omega\tau}\right)^2 \right. \right. \\ & \left. \left. \times \sum_{\alpha=1}^3 \frac{u_\alpha^5}{\prod_{\beta \neq \alpha} (u_\alpha - u_\beta)} \mathcal{Q} \left( \frac{2(\omega + i/\tau)d}{v_F} u_\alpha \right) \right] \right\}, \end{aligned} \quad (20)$$

where  $\mathcal{Q}$  is related to the incomplete gamma function of zeroth order,

$$\mathcal{Q}(x) = \exp(-x)\Gamma(0, -x), \quad (21)$$

and

$$u_1 = \zeta(\mu) + \frac{\mu}{\zeta(\mu)}, \quad u_{2,3} = e^{\pm \frac{2i\pi}{3}} \zeta(\mu) + \frac{e^{\mp \frac{2i\pi}{3}} \mu}{\zeta(\mu)}, \quad (22)$$

with

$$\zeta(\mu) = \sqrt[3]{2i\mu + \sqrt{-\mu^3 - 4\mu^2}}, \quad \mu = \frac{1}{2} \frac{\epsilon_d + \epsilon_m(\omega)}{\epsilon_d + \epsilon_\infty}. \quad (23)$$

In Fig. 3, we compare the predictions of Eq. (20) (colored lines) with the corresponding results of the exact calculations (colored dots), as functions of the distance to the interface, for two different frequencies. Note the excellent agreement in the entire parameter range shown in the figure.

Depending on the relative value of the distance  $d$  and the “electronic” scale  $\ell \equiv v_F \min[\tau, 1/\omega]$ , the analytical expression (21) has the limiting behavior

$$\frac{\Delta\Gamma}{\Gamma_0} = \frac{m_\tau^2 + 2m_n^2}{2|\mathbf{m}|^2} \begin{cases} \gamma_0(\omega, d), & d \ll \ell, \\ \gamma_\infty(\omega, d), & \ell \ll d \ll \lambda_0, \end{cases} \quad (24)$$

where

$$\gamma_0(\omega, d) = \frac{9}{4} \frac{\epsilon_\infty \omega_p^2}{(\epsilon_d + \epsilon_\infty)^2 \omega^3 \tau} \left(\frac{c}{v_F}\right)^2 \frac{c}{\sqrt{\epsilon_d \omega d}}, \quad (25)$$

and

$$\gamma_\infty(\omega, d) = \frac{3}{8} \operatorname{Im} \left[ \frac{\epsilon_m(\omega) - \epsilon_d}{\epsilon_m(\omega) + \epsilon_d} \right] \left( \frac{c}{\sqrt{\epsilon_d \omega d}} \right)^3. \quad (26)$$

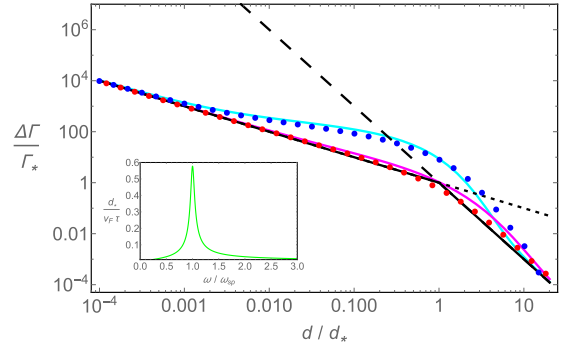


FIG. 3. The spontaneous emission rate as a function of the distance to the interface, in scaled coordinates. The red dots and the red curve correspond to the exact solution and the approximation of Eq. (20) for  $\omega = 0.5\omega_{\text{sp}}$ , while the blue dots and the blue curve show the exact solution and the approximation of Eq. (20) for  $\omega = 2\omega_{\text{sp}}$ . The dipole moment  $\mathbf{m} \parallel \hat{\mathbf{n}}$ . The solid black line corresponds to the interpolation (27), with the black dotted and dashed lines indicating the  $d \ll d_*$  and  $d_* \ll d \ll \lambda_0$  limits of the exact solution. The inset shows the frequency variation of  $d_*$ .

Equation (20) can therefore be further approximated by the interpolating function

$$\Delta\Gamma(d) = \Gamma_* \begin{cases} d_*/d, & d \leq d_*, \\ (d_*/d)^3, & d \geq d_*, \end{cases} \quad (27)$$

where

$$\Gamma_* = \frac{m_\tau^2 + 2m_n^2}{2|\mathbf{m}|^2} \frac{9(c/v_F)^2 \omega_{\text{sp}}^2}{4(\epsilon_d + \epsilon_\infty) \omega^3 \tau} \frac{c}{\sqrt{\epsilon_d \omega d_*}}, \quad (28)$$

and

$$d_* = \frac{1}{\sqrt{3}} \frac{v_F \tau}{\sqrt{1 + (\omega\tau)^2 (1 - \omega_{\text{sp}}^2/\omega^2)^2}}. \quad (29)$$

Here,  $\omega_{\text{sp}}$  is described by the standard expression for the frequency of the surface plasmon resonance at the planar interface of a dielectric with a Drude metal,  $\omega_{\text{sp}} = \omega_p / \sqrt{1 + \epsilon_d/\epsilon_\infty}$ .

The solid black line in Fig. 3 plots Eq. (27), while the dashed and dotted lines correspond to  $\gamma_\infty(\omega, d)$  and  $\gamma_0(\omega, d)$ , respectively. Although not sufficiently accurate at the quantitative level, the interpolation (27) correctly represents the qualitative behavior of the spontaneous emission rate and adequately describes the crossover between the two regimes.

The inset of Fig. 3 shows the frequency dependence of the hyperbolic layer thickness  $d_*$ . Note its nonmonotonic variation, noticed earlier in the context of the general behavior of the spontaneous emission rate as a function of the distance to the interface (see Fig. 1). The regime  $d < d_*$  corresponds to the suppression of the plasmon resonance due to the hyperbolic blockade. Except for  $\omega = \omega_{\text{sp}}$  when  $d_* \sim v_F \tau$ , as a function of frequency  $d_*(\omega)$  behaves as  $v_F/\omega$  at  $\omega > \omega_p$  and as  $v_F \omega/\omega_p^2$  for  $\omega < \omega_p$ , with the characteristic scale given by the Thomas-Fermi screening length  $\sim v_F/\omega_p$ . For a good metal, in the optical range  $d_*$  is on the order of a nanometer. On the other hand, in transparent conducting oxides such as indium tin oxide (ITO) [28] or in doped semiconductors [29,30], we find  $d_*$  on the order of a few tens of nanometers—and the regime  $d < d_*$  corresponds to the common situation of an active quantum

well in close proximity to a doped semiconductor substrate. In this case, the phenomenon of the hyperbolic blockade and the theory introduced in the present work are essential for an accurate accounting of the light emission from such systems.

The predicted hyperbolic blockade and enhanced coupling to hyperplasmonic surface modes are also expected to strongly modify the surface-enhanced Raman scattering (SERS) at a high-quality conductor-dielectric interface. While leaving a detailed discussion of this effect to a future publication [31], it should be noted that its general features are similar to the behavior of the spontaneous emission rate: strong suppression

at and near the surface plasmon resonance frequency due to the hyperbolic blockade, and the enhancement above the surface plasmon resonance frequency due to the coupling to hyperplasmonic modes. This should be contrasted to the existing theories of the SERS at an interface of a nonlocal medium [32,33], which generally focus on the decrease of the SERS intensity due to nonlocality.

This work was partially supported by the National Science Foundation (Grant No. 1629276-DMR), Army Research Office (Grant No. W911NF-14-1-0639), and Gordon and Betty Moore Foundation.

- 
- [1] S. A. Maier, *Plasmonics: Fundamentals and Applications*, 1st ed. (Springer, Berlin, 2007).
- [2] G. W. Ford and W. H. Weber, *Phys. Rep.* **113**, 195 (1984).
- [3] M. Moscovits, Surface-enhanced Raman spectroscopy: A brief perspective, in *Surface-Enhanced Raman Scattering - Physics and Applications*, edited by K. Kneipp, M. Moscovits, and H. Kneipp (Springer, Berlin, 2006).
- [4] I. A. Larkin, M. I. Stockman, M. Achermann, and V. I. Klimov, *Phys. Rev. B* **69**, 121403(R) (2004).
- [5] G. Toscano, J. Straubel, A. Kwiatkowski, C. Rockstuhl, F. Evers, H. Xu, N. A. Mortensen, and M. Wubs, *Nat. Commun.* **6**, 7132 (2015).
- [6] C. Ciraci, R. T. Hill, J. J. Mock, Y. Urzhumov, A. I. Fernández-Dominguez, S. A. Maier, J. B. Pendry, A. Chilkoti, and D. R. Smith, *Science* **337**, 1072 (2012).
- [7] Y. Luo, A. I. Fernández-Dominguez, A. Wiener, S. A. Maier, and J. B. Pendry, *Phys. Rev. Lett.* **111**, 093901 (2013).
- [8] J. Ziman, *Electrons and Phonons: The Theory of Transport Phenomena in Solids* (Oxford University Press, Oxford, UK, 2001).
- [9] E. Narimanov, [arXiv:1712.03484](https://arxiv.org/abs/1712.03484).
- [10] M. A. Noginov, H. Li, Yu. A. Barnakov, D. Dryden, G. Nataraj, G. Zhu, C. E. Bonner, M. Mayy, Z. Jacob, and E. E. Narimanov, *Opt. Lett.* **35**, 1863 (2010).
- [11] Z. Jacob, J. Y. Kim, G. V. Naik, A. Boltasseva, E. Narimanov, and V. M. Shalaev, *Appl. Phys. B* **100**, 215 (2010).
- [12] H. N. Krishnamoorthy, Z. Jacob, E. Narimanov, I. Kretzschmar, and V. M. Menon, *Science* **336**, 205 (2012).
- [13] T. Galfsky, J. Gu, E. E. Narimanov, and V. M. Menon, *Proc. Natl. Acad. Sci. USA* **114**, 5125 (2017).
- [14] L. V. Alekseyev and E. Narimanov, Radiative decay engineering in metamaterials, in *Tutorials in Metamaterials*, edited by M. A. Noginov and V. A. Podolskiy (CRC Press, Boca Raton, FL, 2012).
- [15] G. E. H. Reuter and E. H. Sondheimer, *Proc. R. Soc. London, Ser. A* **195**, 336 (1948).
- [16] E. H. Sondheimer, *Adv. Phys.* **1**, 1 (1952).
- [17] R. G. Chambers, *Nature (London)* **165**, 239 (1950).
- [18] R. G. Chambers, *Proc. R. Soc. London, Ser. A* **215**, 481 (1952).
- [19] In plasmonic metals (such as, e.g., silver, gold, or aluminum) and ceramic materials (e.g., titanium nitride) the field penetration depth is on the order of 50 nm, which is close to the mean free path ( $\sim 50$  nm for silver [34],  $\sim 40$  nm for gold [34],  $\sim 20$  nm for aluminum [34], and  $\sim 45$  nm for titanium nitride [35]). In transparent conducting oxides, with the plasmon resonance in the IR (such as, e.g., indium tin oxide), the field penetration depth is on the order of 100 nm, while the mean free path is  $\sim 20$  nm [36]. In doped semiconductors, with the plasmon resonance in the mid-IR, the field penetration depth is on the order of  $1 \mu\text{m}$ , while the mean free path [29] is  $\sim 100$  nm. None of these plasmonic media operates in the regime of anomalous skin effect.
- [20] R. Kragler and H. Thomas, *Z. Phys. B: Condens. Matter* **39**, 99 (1980).
- [21] K. L. Kliewer and R. Fuchs, *Phys. Rev.* **172**, 607 (1968).
- [22] A. R. Melnyk and M. J. Harrison, *Phys. Rev. B* **2**, 851 (1970).
- [23] K. Fuchs, *Proc. Cambridge Philos. Soc.* **34**, 100 (1938).
- [24] S. B. Soffer, *J. Appl. Phys.* **38**, 1710 (1967).
- [25] J. Khurgin, W.-Y. Tsai, D. P. Tsai, and G. Sun, *ACS Photonics* **4**, 2871 (2017).
- [26] The inequality  $\varepsilon_F \gg k_B T$  is generally well satisfied for plasmonic materials even at room temperature: While  $k_B T \simeq 20$  meV, the Fermi energy is usually on the order of an electron volt.
- [27] G. S. Agarwal and H. D. Vollmer, *Phys. Status Solidi B* **85**, 301 (1978).
- [28] G. V. Naik, V. M. Shalaev, and A. Boltasseva, *Adv. Mater.* **25**, 3264 (2013).
- [29] A. J. Hoffman, L. Alekseyev, S. S. Howard, K. J. Franz, D. Wasserman, V. A. Podolskiy, E. E. Narimanov, D. L. Sivco, and C. Gmachl, *Nat. Mater.* **6**, 948 (2007).
- [30] Y. Zhong, S. Malagari, T. Hamilton, and D. Wasserman, *J. Nanophotonics* **9**, 093791 (2015).
- [31] E. Narimanov (unpublished).
- [32] W. H. Weber and G. W. Ford, *Phys. Rev. Lett.* **44**, 1774 (1980).
- [33] P. T. Leung and W. S. Tse, *Solid State Commun.* **95**, 39 (1995).
- [34] D. Gall, *J. Appl. Phys.* **119**, 085101 (2016).
- [35] J. S. Chawla, X. Y. Zhang, and D. Gall, *J. Appl. Phys.* **113**, 063704 (2013).
- [36] C.-S. Yang, M.-H. Lin, C.-H. Chang, P. Yu, J.-M. Shieh, C.-H. Shen, and O. Wada, *IEEE J. Quantum Electron.* **49**, 677 (2013).